Noncollinear Paramagnetism of a GaAs Two-Dimensional Hole System

L. A. Yeoh,[1] A. Srinivasan,[1] O. Klochan,[1] R. Winkler,[2] U. Zülicke,[3] M. Y. Simmons,[4] D. A. Ritchie,[5] M. Pepper,[6] and A. R. Hamilton[1,*]

[1]School of Physics, University of New South Wales, Sydney, New South Wales 2052, Australia
[2]Department of Physics, Northern Illinois University, De Kalb, Illinois 60115, USA
[3]School of Chemical and Physical Sciences and MacDiarmid Institute for Advanced Materials and Nanotechnology, Victoria University of Wellington, Wellington 6140, New Zealand
[4]Centre for Quantum Computation and Communication Technology, School of Physics, University of New South Wales, Sydney, New South Wales 2052, Australia
[5]Cavendish Laboratory, University of Cambridge, Cambridge CB3 0HE, United Kingdom
[6]Department of Electronic and Electrical Engineering, University College London, London WC1E 7JE, United Kingdom

(Received 6 September 2014; published 3 December 2014)

We have performed transport measurements in tilted magnetic fields in a two-dimensional hole system grown on the surface of a (311)A GaAs crystal. A striking asymmetry of Shubnikov–de Haas oscillations occurs upon reversing the in-plane component of the magnetic field along the low-symmetry $[\bar{2}33]$ axis. As usual, the magnetoconductance oscillations are symmetric with respect to reversal of the in-plane field component aligned with the high-symmetry $[01\bar{1}]$ axis. Our observations demonstrate that an in-plane magnetic field can generate an out-of-plane component of magnetization in a low-symmetry hole system, creating new possibilities for spin manipulation.

DOI: 10.1103/PhysRevLett.113.236401 PACS numbers: 71.70.Ej, 72.20.My, 73.21.Fg, 75.20.-g

Charge carriers in solids behave almost like free electrons, as effects of the crystal lattice can be absorbed into the energy-momentum relations of electronic states associated with the material's band structure. Often, the resulting changes in the carrier dynamics are largely captured by suitably renormalized single-particle parameters such as effective mass, gyromagnetic ratio, and spin-orbit-coupling constant [1]. The advent of nanofabrication techniques has ushered in an era of new opportunities for tailoring the electric and magnetic properties of charge carriers in low-dimensional systems such as quantum wells, wires, and dots [2]. Our work, presented here, reveals unusual properties of quantum-confined valence-band states (i.e., holes) in semiconductor heterostructures [3].

Electrons in the conduction band of typical semiconductors exhibit behavior very similar to free electrons—they carry a negative elementary charge and effective spin-1/2 degree of freedom. Valence band holes are not only different in that they respond like a positively charged particle to an applied electric field, they also typically possess an effective spin 3/2 that is strongly coupled to their orbital motion [1]. As a result, the effective mass of holes in the bulk material depends on the value m_j of the hole's spin projection parallel to the propagation direction: states with $m_j = \pm 3/2$ ($\pm 1/2$) are heavy (light) holes [1,3]. In semiconductor heterostructures, the size-quantization energies of quasi-two-dimensional heavy holes (HHs) and light holes (LHs) differ, and confinement imposes a quantization axis of hole spins parallel to the growth direction (denoted z axis) [3–5]. As both the in-plane motion and the in-plane (i.e., x and y) components of an applied magnetic field are in competition with the HH-LH energy splitting, a rich—and sometimes seemingly counterintuitive—spin-magnetic and spin-electronic behavior is exhibited by 2D hole systems. For example, for the uppermost hole subband, which has HH character near wave vector $\mathbf{k}_\parallel = 0$, the Zeeman splitting linear in an in-plane field is suppressed if the heterostructure is grown in a high-symmetry direction, while a large Zeeman splitting results from a magnetic field applied along the z (growth) direction [6]. Neglecting contributions to Zeeman splitting that depend on the in-plane wave vector $\mathbf{k}_\parallel = (k_x, k_y)$, the coupling of an external magnetic field $\mathbf{B} = (B_x, B_y, B_z)^T$ to the spin of 2D HHs is, thus, given by [5] $H_Z^{(s)} = \frac{1}{2} g_{zz}^* \mu_B B_z \sigma_z$. Here, σ_z is the diagonal Pauli matrix acting in the pseudospin-1/2 space of hole states, with spin projection $\pm 3/2$ (i.e., the HH states), T denotes the transpose of a vector or matrix and g_{zz}^* is the only nonvanishing g factor for 2D holes in a high-symmetry heterostructure. In GaAs, the theoretically predicted value $g_{zz}^* = 7.2$ [3] has recently been experimentally verified [7,8]. However, the situation changes when the quantum well is grown in a low-symmetry crystallographic direction, e.g., on the (311)A surface. In this case, the cubic crystal anisotropy induces a finite B-linear Zeeman splitting even for in-plane fields, which is described by a contribution [3,9]

$$H_Z^{(c)} = \frac{1}{2}\mu_B[(g_{xx}^*\sigma_x + g_{xz}^*\sigma_z)B_x + g_{yy}^* B_y]. \qquad (1)$$

Here, the x and y directions correspond to the $[\bar{2}33]$ and $[01\bar{1}]$ crystallographic axes, respectively. For GaAs, $g_{xx}^* = g_{yy}^* = -0.16$ and $g_{xz}^* = 0.65$ [9].

The existence of a noncollinear term $\propto g^*_{xz}$ implies the possibility to induce an out-of-plane spin polarization by applying an in-plane magnetic field [10]. Here, we provide direct confirmation of the unusual spin polarization associated with g^*_{xz}. Our work constitutes one of the rare occasions where off-diagonal elements in the gyromagnetic tensor $\underline{g}^*$ are accessible for experimental study [11–13].

Samples containing a high-mobility 2D hole system were fabricated from a GaAs/$Al_{0.33}Ga_{0.67}As$ heterostructure grown on a conducting (311)A substrate which doubles as an *in situ* back gate, 2.6 μm away from a symmetrically doped 20 nm wide GaAs quantum well [14]. To detect the out-of-plane spin polarization, we perform transport measurements in tilted magnetic fields within a dilution refrigerator with a base temperature of 25 mK. The sample was mounted on an *in situ* piezoelectric rotator featuring an in-built angle readout mechanism with $\pm 0.01°$ accuracy [15].

To minimize the $B = 0$ Rashba spin splitting due to structural inversion asymmetry, the electric field across the quantum well was tuned via the *in situ* back gate. The optimum operating point was identified as the back-gate bias where beating in the low field Shubnikov–de Haas (SDH) oscillations was minimized, and the classical magnetoresistance dip at $B = 0$ arising from two-band transport was eliminated [16–19]. This symmetric point was found to be $V_{BG} = +1.5$ V, where the 2D hole density was $p = 9.26 \times 10^{10}$ cm^{-2} with a mobility of 0.6×10^6 cm^2 V^{-1} s^{-1} (see Supplemental Material [20] for details). For this experiment, only the lowest 2D HH subband is occupied. To detect the presence of the unusual g^*_{xz} term, we take advantage of the fact that the additional out-of-plane spin polarization created by $g^*_{xz}B_x$ can add to (or subtract from) the out-of-plane spin polarization induced by a perpendicular field $g^*_{zz}B_z$ depending on the relative signs of B_x and B_z. The total spin polarization can then be observed by examining the spin splitting of the SDH oscillations. In this experiment, the magnitudes and relative signs of B_x, B_y, and B_z are controlled by tilting the sample with respect to the magnetic field by some angle θ, shown in Fig. 1(a). We begin by applying the in-plane field along the high symmetry $[01\bar{1}]$ crystal axis, where there is no out-of-plane spin polarization. Figure 1(c) shows the magnetoresistance ρ_{xx} as a function of B_z, for different tilt angles $\pm\theta$. When the field is perpendicular to the quantum well [top trace in Fig. 1(c), $\theta = 0°$], SDH oscillations are observed with no sign of beating at low fields. No spin splitting of magnetoconductance oscillations is observed up to $B_z = 0.25$ T, and there is a well-defined ρ_{xx} minimum at $\nu = 16$ and a ρ_{xx} maximum at $\nu = 17$.

Tilting the sample introduces an in-plane field component B_y along $[01\bar{1}]$, lifting the spin degeneracy of the Landau levels as indicated schematically in Fig. 1(b). This can be seen in the Fig. 1(c) data sets, by following the resistivity at odd filling factors $\nu_{\rm odd}$, such as $\nu = 17$. At

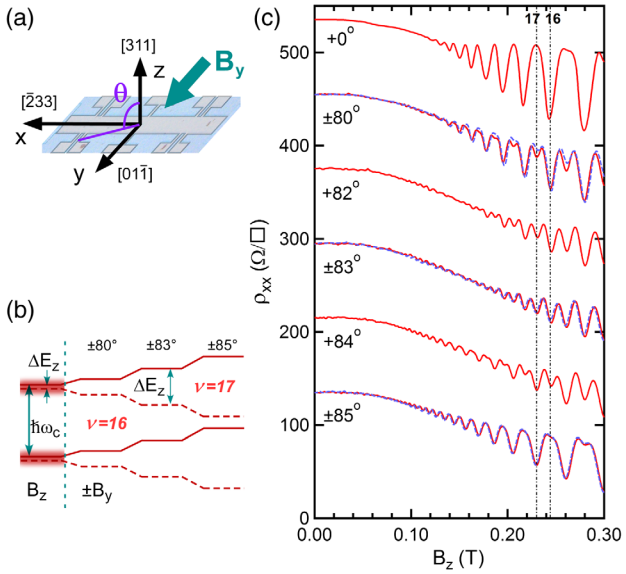

FIG. 1 (color online). (a) Sample orientation and crystal axes with the in-plane field B_y aligned along the $[01\bar{1}]$ axis. (b) Schematic evolution of the Landau levels, beginning with a purely perpendicular field B_z, then increasing the spin splitting by applying an in-plane field B_y, introduced by tilting the sample. (c) Magnetoresistance data for different tilt angles with traces offset vertically by $80\Omega/\square$ for clarity. Solid red lines correspond to $+\theta$ and dashed blue lines to $-\theta$. The vertical dashed lines mark filling factors $\nu = 16$ and $\nu = 17$.

$\theta = 0°$, the nearly spin degenerate Landau levels yield a peak in ρ_{xx}. Tilting to $\theta = \pm 80°$, a weak dip starts to appear and grows stronger with increasing in-plane field, so that by $\theta = \pm 85°$, the ρ_{xx} maximum has evolved into a ρ_{xx} minimum. For even filling factors $\nu_{\rm even}$, the opposite happens, with $\nu = 16$ starting as a well defined ρ_{xx} minimum at $\theta = 0°$ and evolving into a ρ_{xx} maximum at $\theta = \pm 85°$.

As a first approximation, it is tempting to analyze the data and extract g factors using the "coincidence" approach introduced by Fang and Stiles for 2D electrons [25–27]. This method compares the cyclotron energy (dependent on B_z) with the Zeeman splitting (dependent on total field), to extract the product $|g^*m^*|$. However, the coincidence technique assumes parabolic bands (constant m^*) and an isotropic g factor, neither of which is the case for 2D holes. Nevertheless, a crude estimate of the product $|g^*_{zz}m^*|$ can be obtained from the $\theta = 0°$ data by comparing the magnetic field at which the SDH oscillations first become visible ($\Delta\nu_{\rm even} = \hbar\omega_c - g^*_{zz}\mu_B B$ at 0.12 T) with the field at which spin splitting first appears ($\Delta\nu_{\rm odd} = g^*_{zz}\mu_B B$ at 0.35 T). This suggests $g^*_{zz}m^* \sim 0.5$, which is lower than the simple theoretical expectation of $g^*_{zz}m^* = 1.4$ (using $m^* = 0.2$ and $g^*_{zz} = 7.2$ [3]). The reason for this apparent discrepancy is addressed further on in the Letter.

The most striking result of Fig. 1(c) is its similarity to 2D electron systems in that the SDH traces are identical for

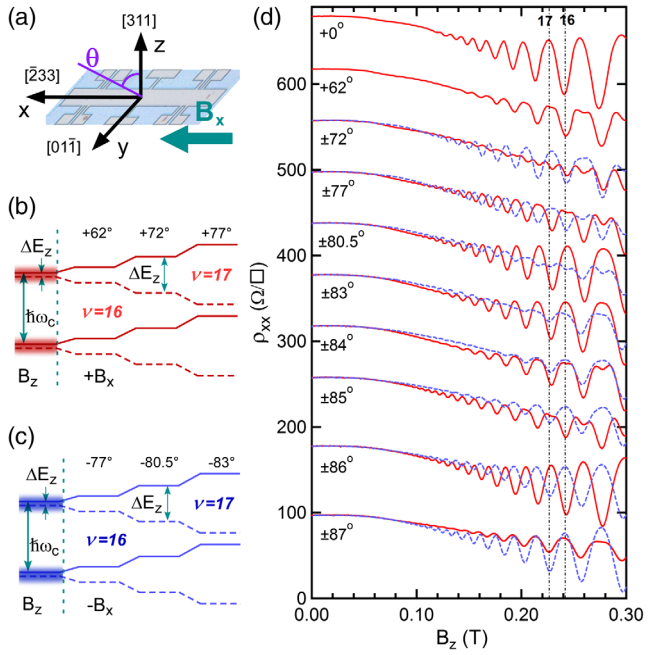

FIG. 2 (color online). (a) Schematic of the sample orientation for the in-plane field B_x aligned along $[\bar{2}33]$. (b) Schematic of the evolution of the Landau levels, starting with perpendicular field B_z, and applying $+B_x$ (red, $+\theta$) and in part (c) applying $-B_x$ (blue, $-\theta$). (d) Magnetoresistance ρ_{xx} for different tilt angles for both $+\theta$ (red solid lines) and $-\theta$ (blue dashed lines). Traces are offset vertically by $40\Omega/\square$ for clarity.

both $+\theta$ and $-\theta$ (solid red and dashed blue traces, respectively), as well as for $+B_y$ and $-B_y$, depicted in Fig. 3(a).

To detect the in-plane-field-induced out-of-plane spin polarization, the sample was thermally cycled and reoriented so that the in-plane field is applied along the low symmetry $[\bar{2}33]$ direction, as shown in Fig. 2(a). The back-gate bias was once again tuned to symmetrize the quantum well, with the symmetry point occurring under similar conditions to the previous cooldown (the back-gate bias differs by 1.3% and the hole density by 0.6%). In this orientation, the effect of the in-plane field on the Landau levels is illustrated in Figs. 2(b) and 2(c). Applying a perpendicular field B_z separates the Landau levels, causing them to split, generating an out-of-plane spin polarization as in the $[01\bar{1}]$ case. However, introducing an in-plane field component B_x generates an additional out-of-plane spin polarization that adds to (or subtracts from) the out-of-plane spin polarization due to B_z. In the case of $+B_x$ (i.e., $+\theta$) shown in Fig. 2(b), the Zeeman splitting is maximized as the $g^*_{zz}B_z$ and $g^*_{xz}B_x$ terms add. In contrast, for $-B_x$ (i.e., $-\theta$) in Fig. 2(c), these terms have opposite signs, resulting in a reduced effective Zeeman splitting. Hence, the spin splitting of the Landau levels evolves much faster for $+\theta$ than $-\theta$.

The top trace in Fig. 2(d) shows the magnetoresistance along $[\bar{2}33]$ in a perpendicular field ($\theta = 0°$), while the remaining SDH traces correspond to an increasing in-plane field component $\pm B_x$, as the sample is tilted to larger $|\theta|$. The most striking feature of this data set is the difference between $+B_x$ (solid red lines for $+\theta$) and $-B_x$ (dashed blue lines for $-\theta$). This difference is most pronounced at high in-plane fields, such as $\theta = \pm 85°$ and $\theta = \pm 86°$, where the SDH oscillations for opposite signs of B_x are completely out of phase with each other. This can only be explained by the out-of-plane spin polarization due to g^*_{xz} as described in Eq. (1).

The impact of the in-plane magnetic field on the Zeeman splitting and Landau level energies can be studied by following the evolution of ρ_{xx} at $\nu = 17$ in Fig. 2(d). At zero tilt angle, the spin splitting is small, leading to a maximum in ρ_{xx}. Beginning with the $-\theta$ traces (dashed blue lines), we can identify three regimes sketched in Fig. 2(c): (i) spin splitting at $\nu = 17$ becomes apparent at $\theta = -77°$, (ii) by $\theta = -80.5°$ the minima at both $\nu = 16$ and $\nu = 17$ are equally well defined, and (iii) for larger tilt angles the ρ_{xx} maximum at $\nu = 17$ evolves into a minimum, while the ρ_{xx} minimum at $\nu = 16$ becomes a maximum. In contrast to $-\theta$, the $g^*_{zz}B_z$ and $g^*_{xz}B_x$ terms add for $+\theta$, and the spin splitting develops more rapidly as a function of $|\theta|$, shown in Fig. 2(b): For $+\theta$ (solid red lines), (i) spin splitting at $\nu = 17$ becomes apparent much earlier at $\theta = +62°$, (ii) by $\theta = +72°$ the minima at $\nu = 16$ and $\nu = 17$ are equally well defined, and (iii) by $\theta = +77°$ the ρ_{xx} maximum at $\nu = 17$ has become a minimum, while the minimum at ρ_{xx} at $\nu = 16$ has become a maximum. Tilting the sample further causes the oscillations to invert a second time at $\theta = +86°$ and again at $\theta = +87°$.

To verify that the difference between $+\theta$ and $-\theta$ stems from the interplay between the g^*_{xz} and g^*_{zz} terms, we check the symmetry of the data with respect to the sign of B_z. In Fig. 3(b), we see that the data are completely symmetric only if the sign of both B_x and B_z are reversed, so that the sign of the ratio B_x/B_z remains the same.

Direct comparison between the tilted-field experimental data and numerical calculations is currently impractical, as the highly complex nature of the hole band structure and the finite width of the 2D system make solving the Hamiltonian with both B_z and $B_\parallel$ components, applied simultaneously, a highly nontrivial task. The band structure of holes for the low-symmetry (311)A surface at zero field is already strongly nonparabolic [28,29]. In our system, the unoccupied HH2 and LH1 energy bands are located -3.64 and -6.06 meV below the HH1 band (located at -0.67 meV), respectively (see Supplemental Material [20] for details). Indeed, there are only a few calculations of the Landau level structure of spin-1/2 electrons with spin-orbit coupling in tilted magnetic fields [30] and none for spin-3/2 holes.

In the case of a purely perpendicular field, the nonparabolicity of the band structure and LH-HH coupling yield a much more complex hole Landau fan diagram compared to electrons. This is shown in Fig. 4(a), obtained

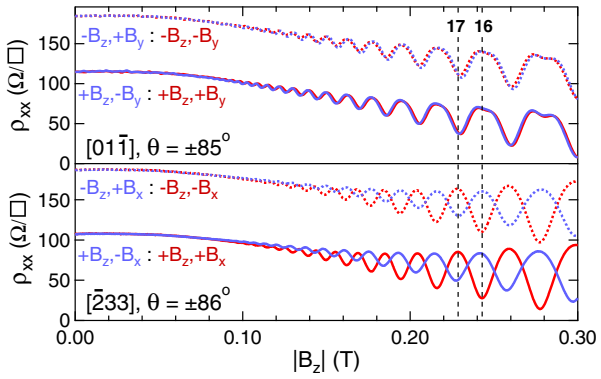

FIG. 3 (color online). Magnetoresistance versus $|B_z|$ comparing the relative orientations of the fields B_i and B_z, where (a) $i = y$, i.e., $\mathbf{B}_\parallel$ along $[01\bar{1}]$ and (b) $i = x$, i.e., $\mathbf{B}_\parallel$ along $[\bar{2}33]$. For each curve the orientations of B_i and B_z are indicated in the figure. Part (a) shows symmetric SDH traces for $\theta = \pm 85°$ in all four cases. In part (b), the traces are distinctly different for $+\theta = \arctan(+B_x/B_z)$ (red) compared to $-\theta = \arctan(-B_x/B_z)$ (blue). Traces in each panel are offset vertically by $70\Omega/\square$.

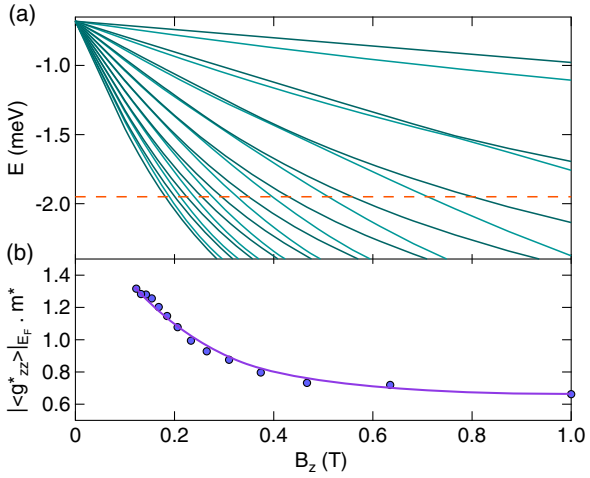

FIG. 4 (color online). (a) Lowest 20 Landau levels for a 20 nm GaAs quantum well in a purely perpendicular field B_z calculated by means of an 8×8 $\mathbf{k} \cdot \boldsymbol{p}$ Hamiltonian. The dashed orange line indicates the Fermi energy at $B = 0$. (b) Product $|g^*_{zz} m^*|$ versus perpendicular field B_z, where g^*_{zz} is extracted from the Zeeman energy gap between adjacent even-odd indexed energy levels around the Fermi energy, and m^* is derived from the cyclotron gap between adjacent odd-odd indexed levels in (a).

from 8×8 $\mathbf{k} \cdot \mathbf{p}$ calculations, taking into account the self-consistent Hartree potential as well as bulk-inversion-asymmetry (Dresselhaus) spin splitting [31]. Here, the total spin splitting ΔE_Z of the Landau levels is highly nonlinear with increasing field. The corresponding product $|g^*_{zz} m^*|$, extracted from the energy gaps between Landau levels at the Fermi energy is given below in part (b). Here, m^* has been derived from the cyclotron gap for a given $\Delta\nu_{\text{even}}$, and g^*_{zz} is the averaged value calculated from the adjacent Zeeman gaps $\Delta\nu - 1$ and $\Delta\nu + 1$. The calculations show that the effective g factor determined from the Zeeman energy gap between even and odd index Landau levels, $\Delta E_Z = g^*_{zz} \mu_B B_z$ decreases from $|g^*_{zz} m^*| = 1.32$ ($g^*_{zz} = 6$, $m^* = 0.22$) at $B_z = 0.12$ T to $|g^*_{zz} m^*| = 0.88$ ($g^*_{zz} = 3.7$, $m^* = 0.23$) at 0.3 T, in Fig. 3(b). This explains why the product $g^*_{zz} m^* \sim 0.5$ obtained from the experiments at $\theta = 0°$ is lower than the value predicted by simple theory, although it is in good agreement with Fig. 4 which trends to $g^*_{zz} m^* \sim 0.6$ at higher fields.

Despite the challenge of performing a quantitative comparison between experiment and theory, we are able to compare the sign of the out-of-plane spin polarization with theory, assuming adiabatic spin dynamics, where the $\mathbf{k} \cdot \mathbf{p}$ calculations for our data show that both g^*_{zz} and g^*_{xz} are positive (theory gives $g^*_{zz} = 7.2$, $g^*_{xz} = 0.65$ [5]). From the tilted-field experiments, with $B_\parallel$ applied along the $[\bar{2}33]$ axis, we find a larger spin splitting for $+\theta$ than $-\theta$; i.e., g^*_{xz} and g^*_{zz} have the same sign, which is consistent with theory.

In conclusion, we report the direct observation of an out-of-plane spin polarization of itinerant 2D holes generated by an in-plane magnetic field. This phenomenon is unique to 2D holes formed in a low-symmetry zinc blende crystal structure such as GaAs, and stems from the interplay between the quantum-well confinement and lattice symmetries. We have determined the relative signs of the g^*_{xz} and g^*_{zz} components in the g tensor and shown these to be consistent with 8×8 $\mathbf{k} \cdot \mathbf{p}$ calculations. This work demonstrates a unique way to manipulate the perpendicular spin polarization without coupling to the orbital momentum, paving the way for more detailed studies and applications of noncollinear magnetic responses in low-dimensional hole systems.

We thank A. Edgar, T. Li, O. P. Sushkov, and G. Vignale for invaluable discussions, J. Cochrane and A. P. Micolich for technical support. This work was supported by the Australian Research Council (ARC) under the Discovery Projects (DP) scheme and by the NSF under Grant No. DMR-1310199. A. R. H. acknowledges support from an ARC Discovery Outstanding Researcher Award (DORA).

*Alex.Hamilton@unsw.edu.au

[1] P. Y. Yu and M. Cardona, *Fundamentals of Semiconductors*, 2nd ed. (Springer, Berlin, 1999).
[2] D. Awschalom, Physics **2**, 50 (2009).
[3] R. Winkler, *Spin-Orbit Coupling Effects in Two-Dimensional Electron and Hole Systems*, (Springer, Berlin, 2003).
[4] K. Suzuki and J. C. Hensel, Phys. Rev. B **9**, 4184 (1974).
[5] R. Winkler, D. Culcer, S. J. Papadakis, B. Habib, and M. Shayegan, Semicond. Sci. Technol. **23**, 114017 (2008).
[6] H. W. van Kesteren, E. C. Cosman, W. A. J. A. van der Poel, and C. T. Foxon, Phys. Rev. B **41**, 5283 (1990).
[7] A. Srinivasan, L. A. Yeoh, O. Klochan, T. P. Martin, J. C. H. Chen, A. P. Micolich, A. R. Hamilton, D. Reuter, and A. D. Wieck, Nano Lett. **13**, 148 (2013).

[8] F. Nichele, S. Chesi, S. Hennel, A. Wittmann, C. Gerl, W. Wegscheider, D. Loss, T. Ihn, and K. Ensslin, Phys. Rev. Lett. **113**, 046801 (2014).
[9] R. Winkler, S. J. Papadakis, E. P. De Poortere, and M. Shayegan, Phys. Rev. Lett. **85**, 4574 (2000).
[10] Throughout this Letter, "spin polarization" refers to the pseudospin-1/2 space of HH states.
[11] A. Abragam and B. Bleaney, *Electron Paramagnetic Resonance of Transition Ions* (Clarendon, Oxford, 1970).
[12] L. F. Chibotaru, A. Ceulemans, and H. Bolvin, Phys. Rev. Lett. **101**, 033003 (2008).
[13] Physical quantities related to Zeeman energy splitting generally depend upon the square $\underline{g}^* \cdot \underline{g}^{*T}$ of the g tensor, which normally mixes off-diagonal elements in an inextricable way [11]. The particular properties of $\underline{g}^*$ for a (311)A-grown quantum well, and the reasons why g^*_{xz} becomes directly observable in our experiment, are discussed in greater detail in the Supplemental Material [20].
[14] M. Y. Simmons, A. R. Hamilton, S. J. Stevens, D. A. Ritchie, M. Pepper, and A. Kurobe, Appl. Phys. Lett. **70**, 2750 (1997).
[15] L. A. Yeoh, A. Srinivasan, T. P. Martin, O. Klochan, A. P. Micolich, and A. R. Hamilton, Rev. Sci. Instrum. **81**, 113905 (2010).
[16] J. P. Eisenstein, H. L. Stormer, V. Narayanamurti, A. C. Gossard, and W. Wiegmann, Phys. Rev. Lett. **53**, 2579 (1984).
[17] S. S. Murzin, S. I. Dorozhkin, G. Landwehr, and A. C. Gossard, JETP Lett. **67**, 113 (1998).
[18] A. R. Hamilton, M. Y. Simmons, M. Pepper, and D. A. Ritchie, Aust. J. Phys. **53**, 523 (2000).
[19] S. J. Papadakis, E. P. De Poortere, H. C. Manoharan, M. Shayegan, and R. Winkler, Science **283**, 2056 (1999).
[20] See Supplemental Material at http://link.aps.org/supplemental/10.1103/PhysRevLett.113.236401, which includes Refs. [21–24], for additional data and calculations.
[21] J. R. Pilbrow and M. R. Lowrey, Rep. Prog. Phys. **43**, 433 (1980).
[22] A. B. Roitsin, Phys. Status Solidi B **104**, 11 (1981).
[23] J. F. Nye, *Physical Properties of Crystals*, 2nd ed. (Clarendon, Oxford, 1985).
[24] R. K. Hayden, L. Eaves, M. Henini, E. C. Valadares, O. Kühn, D. K. Maude, J. C. Portal, T. Takamasu, N. Miura, and U. Ekenberg, Semicond. Sci. Technol. **9**, 298 (1994); R. K. Hayden, E. C. Valadares, M. Henini, L. Eaves, D. K. Maude, and J. C. Portal, Phys. Rev. B **46**, 15586 (1992).
[25] F. F. Fang and P. J. Stiles, Phys. Rev. **174**, 823 (1968).
[26] R. J. Nicholas, R. J. Haug, K. V. Klitzing, and G. Weimann, Phys. Rev. B **37**, 1294 (1988).
[27] S. J. Papadakis, E. P. De Poortere, and M. Shayegan, Phys. Rev. B **59**, R12743 (1999).
[28] R. K. Hayden, E. C. Valadares, M. Henini, L. Eaves, D. K. Maude, and J. C. Portal, Phys. Rev. B **46**, 15586 (1992).
[29] E. C. Valadares, Phys. Rev. B **46**, 3935 (1992).
[30] W. Desrat, F. Giazotto, V. Pellegrini, M. Governale, F. Beltram, F. Capotondi, G. Biasiol, and L. Sorba, Phys. Rev. B **71**, 153314 (2005).
[31] G. Dresselhaus, Phys. Rev. **100**, 580 (1955).